

**Lithium-Ion Battery Thermal Management Systems Using Flexible Graphite Heat
Dissipators**

Thesis

Presented in Partial Fulfillment of the Requirements for Graduation with Distinction in
the Mechanical Engineering Department of The Ohio State University

By

Matthew George Myers

Baccalaureate Program in Mechanical Engineering

The Ohio State University

May 2012

Thesis Examination Committee:

Dr. Yann Guezennec, Advisor

Marcello Canova, Co-Advisor

Copyright by
Matthew George Myers
2012

Abstract

Lithium-Ion batteries are used in a wide variety of devices over a broad range of powers. All batteries generate heat due to the internal resistance of the battery and entropic effects which is roughly proportional to amount of power being drawn from the cells. This heat can cause many problems in the operation of the battery including shortening the lifetime of the cells, reducing their power output, electrical imbalance between the cells due to non-uniform heating within a pack, and even the possibility of fire and explosion in extreme cases. Thermal management of the cells then becomes an important study. As technology progresses, higher power demands are put onto the battery packs. In addition, cells are routinely packed together as tightly as possible to conserve space. This increasing power density demands that heat be shared evenly between individual cells and ultimately removed from the battery pack. This research investigates the application of flexible graphite material in managing the heat production of lithium ion battery packs.

The pack chosen for this study is a 10 cell, 36 volt pack consistent with the type found in modern hand-held rechargeable power tools. Three packs were designed including a control and two packs with different heat spreader geometries. The packs were constructed and instrumented with voltage leads on the individual cells and thermocouples. The packs were then subjected to a series of high-current charge/discharge cycles. Deviations in the voltages of the cells and the temperatures at several points within each pack were monitored as the batteries were cycled. When a

predetermined exit condition based on a maximum limit on voltage and temperature spread within a pack, the experiment was concluded.

While there was not enough data as of yet to detect a significant slowdown in voltage imbalance increase, there did appear to be a reduction in the rate of increase in temperature imbalance by using the graphite heat spreaders that should lead to an improvement in endurance as the experiment progresses.

Acknowledgements

There are several people I would like to offer my thanks to for helping me to complete my research and this thesis. Dr. Yann Guezennec has my heartfelt thanks for taking me on as an undergraduate researcher at the eleventh hour and for helping me keep on schedule. I am also grateful for the funding and support provided by GrafTech International, without whose support this research would not have been possible. Dr. Marcello Canova, Hussam Khasawneh, John Neal and Jim Shively have my sincere gratitude as well for their time, technical support and advice. I would also like to acknowledge the support and effort of Dr. Robert Siston who has greatly expanded my public speaking skill-set. Finally I would like to thank the rest of the staff at the Center for Automotive Research in making it possible for me to have access to the facilities at CAR and to conduct my research.

Table of Contents

Abstract	ii
Acknowledgements	iv
Table of Contents	v
List of Figures	vii
List of Tables	viii
Chapter 1: Introduction	1
1.1: Focus of Thesis	1
1.2: Significance of Research	1
1.3: Overview of Thesis	3
Chapter 2: Background Information	5
2.1: Development of Lithium Ion Cells	5
2.2: Characteristics of Lithium Ion Cells	5
2.3: Battery Overheating Issues	7
2.4: Current Battery Thermal Management	11
2.5: Need for Thermal Management Alternatives	12
2.6: Flexible Graphite Development and Properties	13
2.7: Suitability of Graphite as a Thermal Management System	14
Chapter 3: Previous Research	16
3.1: GrafTech	16
3.2 Center for Automotive Research at The Ohio State University	18
Chapter 4: Methods and Procedure	21
4.1: Experiment Overview	21

4.2: Problems with Original Pack Design	21
4.3: Design and Construction of New Packs	23
4.4: Testing apparatus	28
4.5: Test parameters	33
Chapter 5: Results	35
Chapter 6: Conclusion	35
6.1: Contributions	42
6.2 Future Work	42
6.3 Summary	43
References	44

List of Figures

Figure 1: Structure of cylindrical lithium-ion cell	6
Figure 2: Power and energy densities for several energy solutions	7
Figure 3: Results of battery fires	8
Figure 4: Thermal managed battery pack	9
Figure 5: Thermally unmanaged battery pack	10
Figure 6: Typical discharge curve for a three cell battery pack	11
Figure 7: Lithium-ion battery from the Nissan Leaf	11
Figure 8: Liquid cooled Tesla Roadster Battery	12
Figure 9: Structure of crystalline graphite	13
Figure 10: Flexible graphite material	14
Figure 11: Diagram of GrafTech simulated cells with cooling setup	16
Figure 12: Results of GrafTech simulated battery cooling experiment	17
Figure 13: Thermographs of GrafTech battery cooling experiment	17
Figure 14: Battery pack configuration	18
Figure 15: Comparison of experimental and predicted temperatures	19
Figure 16: Thermograph comparison simulated and experimental results	20
Figure 17: A123 cell and specifications	21
Figure 18: Arrows showing flexible graphite adhesive failure	22
Figure 19: CAD model of new battery pack design	23
Figure 20: Components of new battery pack design	24
Figure 21: Routing of graphite material	25
Figure 22: Top view of pack 2 prior to heat sink addition	26

Figure 23: Top view of pack 3 heat spreaders	27
Figure 24: Locations of battery pack thermocouples	27
Figure 25: Completed test pack connected to testing setup	28
Figure 26: Maccor battery testing system	29
Figure 27: User interface for Maccor tester	30
Figure 28: User interface for the data acquisition system	31
Figure 29: Overall system data flow	32
Figure 30: Image of complete experimental setup	32
Figure 31: Charge/discharge cycle flowchart	33
Figure 32: Maximum cell difference vs. time	35
Figure 33: Cell standard deviation as a function of time	36
Figure 34: Plot of the maximum thermocouple difference	37
Figure 35: Plot of the thermocouple standard deviation	38
Figure 36: Pack 1 voltage traces for preliminary 7 cycles	39
Figure 37: Pack 1 temperature traces for preliminary 7 cycles	39
Figure 38: Maximum cell voltage difference vs. cycle for all packs	40
Figure 39: Maximum temperature imbalance for all packs	41

Chapter 1: Introduction

1.1: Focus of Thesis

This thesis focuses on a relatively new method for the cooling and thermal management of lithium-ion battery packs. A material called flexible graphite, sold under the trade name Spreadershield™ by GrafTech International, will be installed into several test packs and the effect on cell performance and endurance investigated.

1.2 Significance of Research

Lithium-Ion batteries greatly outperform previous technologies using chemistries such as nickel-metal hydride and nickel-cadmium. This performance has led to these batteries becoming ubiquitous in our everyday lives. Lithium-ion batteries are used in cell phones, computers, power tools, and have recently made the move into production automobiles and even some light experimental aircraft. More and more attention is now being focused on improving the performance and safety of these batteries. One of the key factors in this effort is the management of heat.

Heat is produced in a battery from both resistive “joule heating” and from entropic effects. When this heat is not removed, it causes a variety of problems. A thermal imbalance between cells will cause a resulting charge imbalance, which will limit the amount of charge that can be drawn from a pack. Overheating cells can also degrade the cell, shortening its life and power output. In extreme cases, overheating can lead to physical cell damage which could cause the battery to catch fire or explode.

There are currently several methods being used to try and control the heat output in lithium ion batteries. These methods include active and passive air cooling, liquid

cooling, refrigerant cooling, and the use of heat pipes. All of these solutions share a common problem however, which is weight. One of the weaknesses of using batteries as power sources is their relatively low power and energy densities. Any weight added for cooling systems further reduces this power density. Even using aluminum in these heat management systems can cause the weight of the battery to rule it out for some applications. Lighter weight heat management solutions are therefore needed to make lithium ion batteries a viable option for certain uses.

GrafTech International, which manufactures many graphite based materials, has proposed the use of a flexible graphite material as a possible solution to challenge of light weight thermal management systems for lithium-ion batteries. Graphite is 30% lighter than aluminum and has a higher thermal conductivity in the direction of the crystalline planes^[2]. It is also thin and flexible, which can lead to higher power to volume ratios for the batteries. It is produced in large quantities and is easily applied to most surfaces. For very high power uses, the flexible graphite could be used in conjunction with other heat management methods, serving as a way to transport heat away from the center of a large battery pack to an external heat sink.

Preliminary research has already been done at GrafTech and the Center for Automotive Research (CAR) here at The Ohio State University with promising results. Using resistive heaters to simulate batteries, GrafTech has found that flexible graphite heat spreaders provided a 27% higher heat transfer coefficient than a similar aluminum spreader, as well as a 38% decrease in peak temperature under transient conditions. The flexible graphite construction also weighed 28% less than the aluminum which would increase pack specific power and energy^[2].

The Center for Automotive Research at The Ohio State University performed computer simulations and ran experiments on two heat spreader configurations and found that the flexible graphite was effective at decreasing peak cell temperature and increasing temperature uniformity.

These results were promising, but more research and experimentation needed to be done to investigate whether or not a thermal management system using flexible graphite heat spreaders would be able to show a significant improvement in battery performance and endurance.

1.3: Overview of Thesis

This thesis continues this previous research and aims to determine the efficacy of a flexible graphite based lithium-ion battery thermal management system in improving the endurance and overall lifetime of the pack. The cells used for the evaluation of the cooling system are the same cells used in the previous CAR study and are typical in type and number to the cells used in commercial hand-held power tools.

This study begins with the design, construction and instrumentation of two new battery packs using two different geometric configurations of the flexible graphite material. A third pack is carried over from the previous CAR experiments and is used as a non-thermally managed control. The packs are then balanced to ensure a baseline starting point with minimal cell unbalance. The packs are then cycled by charging and discharging under a selected current profile. The packs continue to cycle until an exit condition is reached by one of the packs based on temperature and voltage divergence between an individual pack's cells. The final imbalance in all the battery packs is finally evaluated and a correlation sought between pack aging and thermal management.

This thesis will begin with an overview of lithium-ion cells, including their advantages, disadvantages and need for thermal management. Next, the flexible graphite material provided by GrafTech will be examined in closer detail in chapter 3. Chapter 4 will take a look at the preliminary research conducted both by GrafTech and also by Center for Automotive Research at The Ohio State University. Then, in chapter 5, the experiments conducted to evaluate the flexible graphite's effect on pack performance and endurance will be fully described. The results of this experiment will be detailed as well. Finally, chapter six will then provide the conclusions and future recommendation of this study.

The overall goal of this study is to evaluate the effect of a lithium-ion battery back thermal management system based on a flexible graphite material produced by GrafTech Industries on battery pack performance and endurance.

Chapter 2: Background Information

2.1: Development of Lithium Ion Cells

Lithium-ion batteries are a relatively new rechargeable battery chemistry. Early research on lithium based batteries started in the mid 1970s at academic institutions and over the next decade the technology was developed and refined^[5]. The first commercial lithium-ion battery wasn't released until 1991^[5] by Sony and Asahi Kasei (a Japanese materials science company). Over the next twenty years, the technology was quickly improved and soon out-performed other battery types such as nickel cadmium and nickel metal-hydride. Because of their superior performance and constant improvement across the board, they soon became the largely dominant rechargeable battery across industries including personal electronic devices, hand-held power tools, electric and hybrid vehicles, and even a couple experimental electric aircraft.

2.2: Characteristics of Lithium Ion Cells

Lithium-ion batteries, like most batteries, consist of a positive and negative electrode separated by a liquid electrolyte which allows the free passage of ions. In a typical modern lithium-ion battery, the negative terminal, or anode, is made from a carbon compound, usually graphite. The cathode, or positive terminal is constructed of a lithium-metal oxide compound, for example lithium-iron phosphate. The electrolyte is composed of complexed lithium salts dissolved in a non-aqueous solvent. (Water is not used as lithium metal reacts strongly with water and poses a safety risk.) As the cell discharges, lithium ions are transferred from the anode to the cathode, and as the cell is charged the ions migrate back to the cathode. Figure 1 below shows the general

structure of a cylindrical lithium-ion cell, as well as a schematic showing ion and current flow.

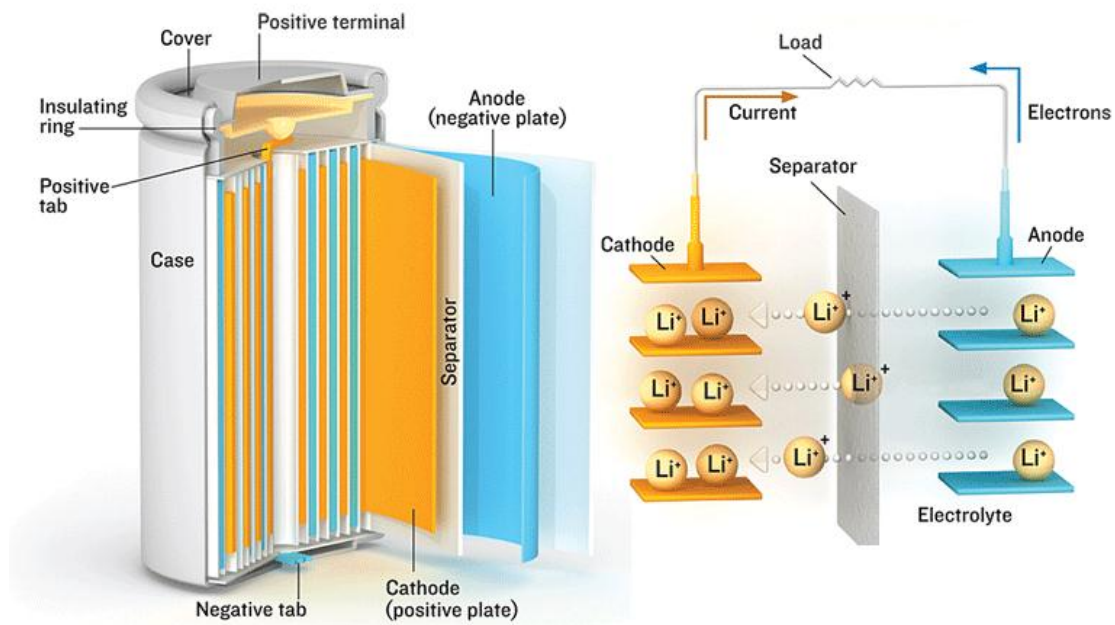


Figure 1: Structure of cylindrical lithium-ion cell¹

The advantages of these cells and the reason these batteries have become so popular is that they possess several distinct advantages over other battery chemistries. A large part of this is their superior power density and energy density. Power density is the amount of power that can be delivered by a system divided by that systems mass (W/Kg in SI units) and energy density is the total amount of energy stored in a system divided by the systems mass (J/Kg in SI units.) Simply put, given two batteries of similar size and weight, the lithium-ion battery will hold more charge at higher energy, and also deliver that energy at a faster rate. Figure 2 below shows the power and energy density of several different energy storage devices. Note that lithium-ion

¹ <http://spectrum.ieee.org/images/sep07/images/lithf2.gif>

batteries are shown at the leading edge of battery technology, but also note that they still fall short of internal combustion engines. In addition, lithium-ion batteries do not suffer from a “memory-effect” which is an effect which can cause losses in cell capacity over time when the pack is not completely discharged before recharging. Lithium-ion batteries also have a low self-discharge rate compared to other battery chemistries and will not lose a significant amount of charge when left to sit for a number of weeks.

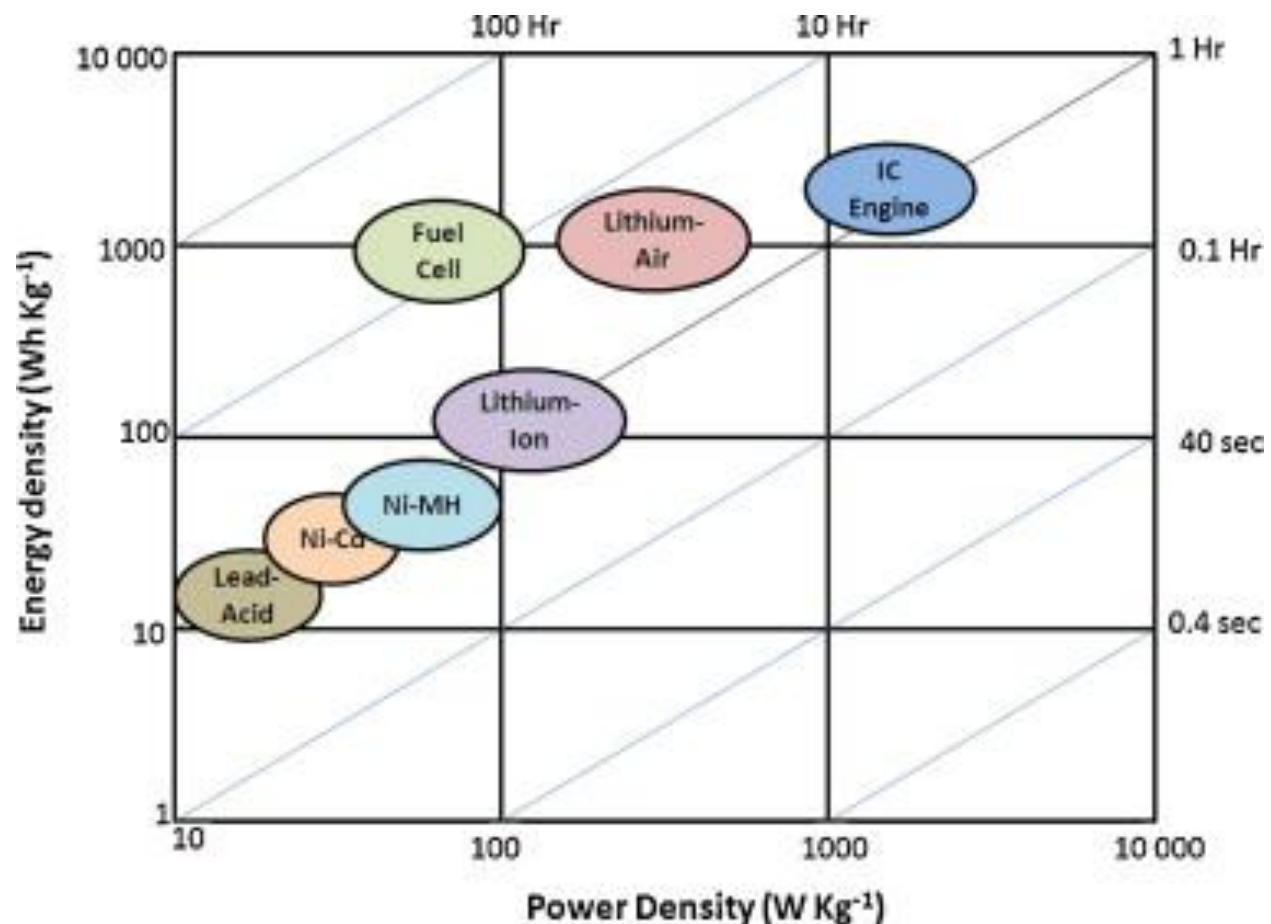


Figure 2: Power and energy densities for several energy storage solutions²

Lithium-ion batteries are not perfect, however and do suffer from several disadvantages. Probably the biggest disadvantage is their susceptibility to temperature.

² <http://ars.els-cdn.com/content/image/1-s2.0-S0378775311001108-gr2.jpg>

2.3: Battery Overheating Issues

The high power density of lithium-ion batteries turns out to be a bit of a double-edged sword. Because no energy storage and delivery system is perfectly efficient, any increase in power output is accompanied by an increase in waste heat. This heat comes from both the chemical reactions in the cell, and the joule heating caused by the current flow through the batteries intrinsic internal resistance. Having a high power to weight ratio then means producing more heat in less mass, which means less material to store the heat in. All this translates into cells that heat up faster and attain higher temperatures than other cell chemistries. Lithium-ion batteries, however, do not respond well to high temperatures. Overheating causes several problems including shortened lifetime, charge imbalance between the cells in the battery, decreased power output, and in extreme cases fire or explosion. Figure 3 below shows the results of several batteries that have undergone thermal runaway.



Figure 3: Results of battery fires³

³ http://priuschat.com/forums/attachments/prius-hybrid-ev-alt-fuel-news/10650d1216925442-prius-a123-battery-fire-report-prius_a123.jpg

Thermal management then becomes an important issue when dealing with high power applications of lithium-ion batteries.

The ideal operating temperature range for lithium-ion batteries is between 20-40°C. If the cells are operated outside this range for extended periods of time, the endurance of the battery pack can be significantly reduced. This can be due to damage to the individual cells, or by imbalance between the cells in the battery pack.

As temperature increases, the rates of chemical reactions tend to increase. The aging of a battery pack is due to unwanted chemical reactions occurring alongside the reactions that produce the electric power. These unwanted chemical reactions cause the capacity of a cell to drop and the internal resistance of a cell to increase. Any increase in temperature will then accelerate this aging process and reduce the useful life of the cell.

An imbalance in temperature can reduce the lifetime of a battery pack even further. Consider two battery packs that both generate an equal amount of heat, with one pack thermally equalized and the other with a significant temperature gradient. The pack that is thermally equalized by the use of heat spreaders has the heat distributed among all the cells in the pack, and therefore thermal aging is shared by all the cells as depicted in figure 4 below.

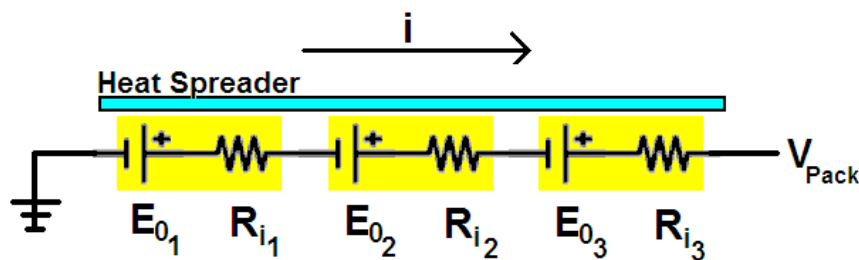


Figure 4: Thermal managed battery pack

In the pack with no thermal management, some cells become hotter than others, meaning that some cells age faster than others. Because the cells in a pack are often arranged in series to increase the voltage of a certain battery chemistry, the current through all the cells is the same, so that if one cell reaches a zero SoC before the others, the pack becomes unusable. Figure 5 shows an unmanaged pack.

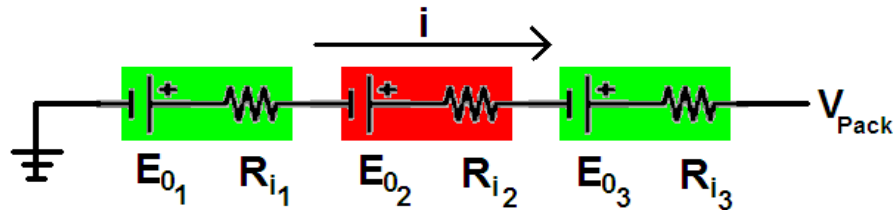


Figure 5: Thermally unmanaged battery pack

Another way to say this is that the battery is only as strong as its weakest cell. Without thermal management, some cells become hotter than the cells in the equivalent pack with thermal management, and because the pack is only as strong as its weakest cell, the thermally unmanaged battery pack loses capacity faster.

The capacity is limited largely due to voltage requirements. Lithium Ion packs will start to severely overheat or become irreversibly discharged if they are drained much below two volts. If there is a voltage imbalance due to a thermal imbalance, the most degraded cell will reach the cut-off voltage first and use of the pack must be terminated. Figure 6 illustrates this by use of a typical discharge curve for an unbalanced 3-cell battery pack. As shown below, when cell 3 reaches the cut-off voltage, its usable capacity is shown on the x axis directly below where the discharge curve intersects the cut-off voltage. The other two cells still have a usable capacity, but this capacity is inaccessible as further discharging the battery pack would result in cell 3 falling to dangerously low voltages.

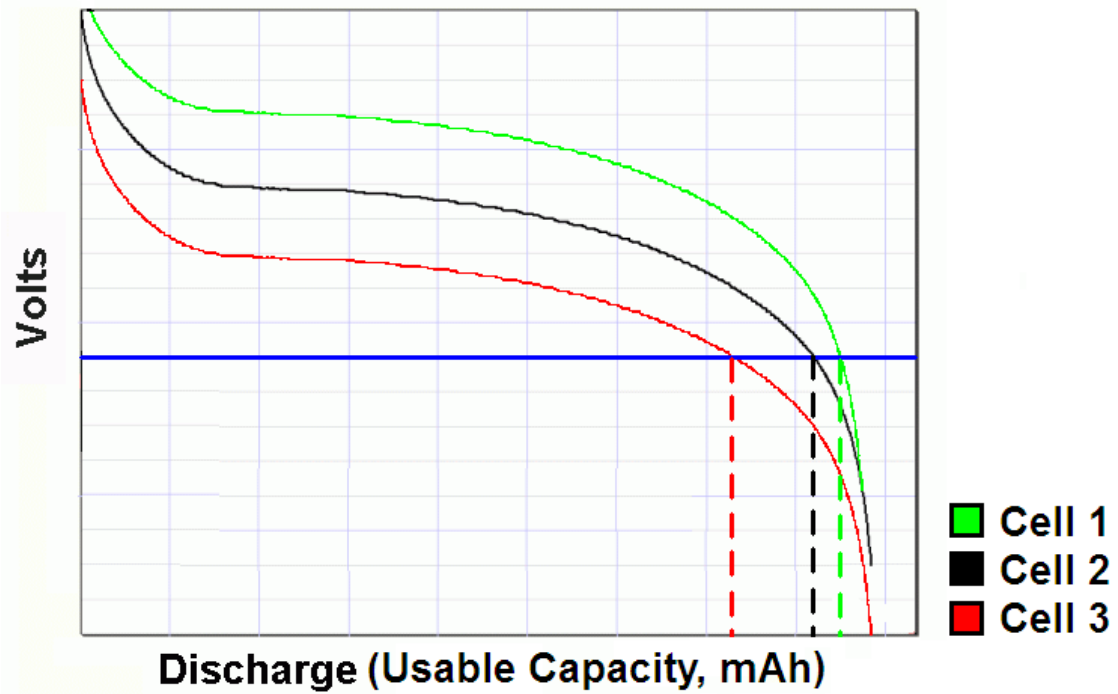


Figure 6: Typical discharge curve for a three cell battery pack

2.4: Current Battery Thermal Management

Many solutions have been devised for temperature management in lithium-ion battery packs. The simplest solution is just a passive air cooling system such as that used in the Nissan Leaf lithium-ion battery system shown below in figure 7.



Figure 7: Lithium-ion battery from the Nissan Leaf^[2]

This, however, has raised some eyebrows in the automotive engineering community as under-engineered, and the CEO of Tesla motors even describes it as “primitive”. Other more powerful cooling systems include active air cooling with aluminum heat spreaders, liquid cooling systems, and refrigerant cooling systems. Shown in figure 8 below is the battery pack from a Tesla Roadster which utilizes an proprietary active liquid cooling system.



Figure 8: Liquid cooled Tesla Roadster Battery⁴

This type of cooling system is much more effective at removing waste heat from the lithium-ion cells and keeps them running stronger and longer, however these more advanced cooling systems are not without their problems.

2.5 Need for Thermal Management Alternatives

The liquid cooled systems come with reliability and maintenance concerns due to the possibility of leaks and pump failures. All of the actively cooled systems reduce the available power from the pack slightly due to operation of pumps and fans. And even the passively cooled aluminum heat spreader solutions share the major problem common to all of these cooling solutions. That problem is weight. Referring back to

⁴ <http://www.teslamotors.com/roadster/technology/battery>

figure 2, while lithium-ion batteries are at the forefront of secondary battery technology, they are far behind the kinds of power and energy densities that internal combustion engines are capable of. Any extra weight added to the battery system drops their power and energy densities even lower and makes it more difficult for them to compete with other technologies. It is important, then, to find a cooling solution that is not only effective, but also very light in weight.

2.6: Flexible Graphite Development and Properties

Flexible graphite is the material used in the GrafTech Spreadershield™ line of heat spreaders. It is a material derived from graphite, whose structures is shown in figure 9 below, and shares with it the anisotropic thermal properties of that material.

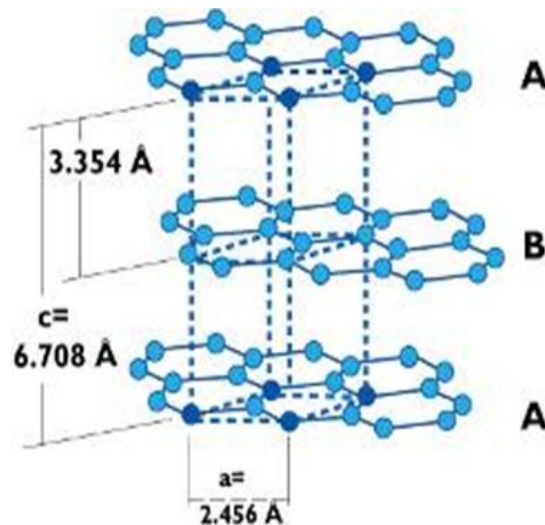


Figure 9: Structure of crystalline graphite^[2]

Due to the tight lattice structure within the horizontal planes shown, phonons (discrete quanta of vibration) travel readily and efficiently which leads to a high thermal conductivity in this direction. In addition, the conjugated p-orbitals in these planes lead to high electrical conductivity along the same planes which would lead to a high

electrical component of thermal conductivity, although this effect is probably overshadowed by the vibrational contributions. This leads to an in-plane conduction of anywhere from 300-1500 W/mK, with a crossplane conduction of 6-16 W/mK. The material has a density of between 1.3-2.2 g/cm³ and can be produced in sheets between 0.025 and 1 mm thick.

The material is also very flexible and can be bent around small radii and bent around corners. It is able to be produced in large quantities and can be die-cut into any planar shape, and can also be manufactured with a pre-applied adhesive backing. Figure 14 shows meter-wide rolls of the stock material, as well as some smaller cut-outs.



Figure 10: Flexible graphite material^[2]

2.7: Suitability for a Thermal Management System

These characteristics of the flexible graphite make it an ideal solution for thermal management in lithium-ion battery packs as it is lightweight and has a high thermal conductivity. It is around 30% less dense than aluminum, has at least a 20% higher

thermal conductivity (in-plane). It's flexibility allows it to be easily threaded in between the cells of a battery pack without any special tooling needed for shaping, and the adhesive backing allows construction without and fasteners or welding.

Chapter 3: Previous Research

3.1: GrafTech

GrafTech Industries conducted an experiment to evaluate the effectiveness of their flexible graphite material in removing heat from flat prismatic cells compared to heat spreaders made from aluminum. The experiment consisted of several simulated batteries constructed from 1/8 inch thick aluminum plates approximately 8x6 inches in dimension. To these plates were affixed 2 80W Kapton Heaters measuring 2x8 inches. A water cooling pipe was wrapped around 3 edges of the cells. One cell was fitted with aluminum heat spreaders on the faces of the cells to conduct heat from the large surface to the cooling pipe on the periphery, and the other was fitted with graphite heat spreaders. A schematic of the setup is shown below in figure 11.

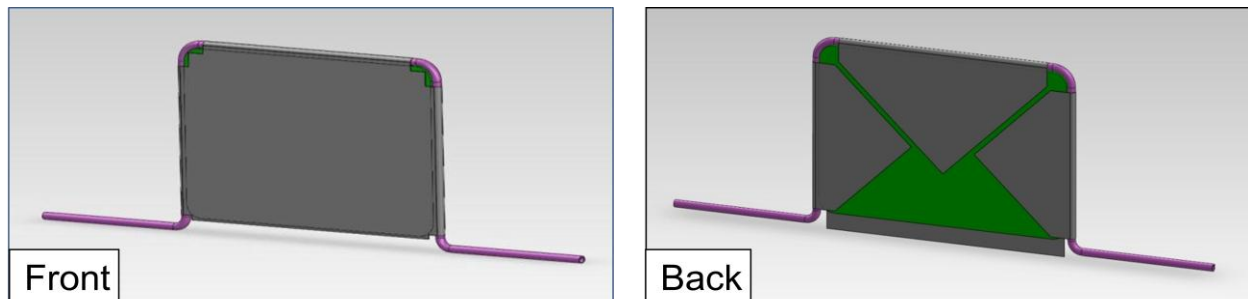


Figure 11: Diagram of GrafTech simulated cells with cooling setup^[2]

A control with no heat spreaders and only a peripheral cooling pipe was also tested. Thermocouples were affixed to monitor the simulated cells, and a thermal imaging camera was also used.

At the start of the test, the heaters were powered at 21W. Four hundred seconds after the heaters were activated, water at 15°C was pumped through the peripheral cooling pipe. Data was then taken every 10 seconds for a period of thirty minutes. The results are shown in figures 12 and 13 below.

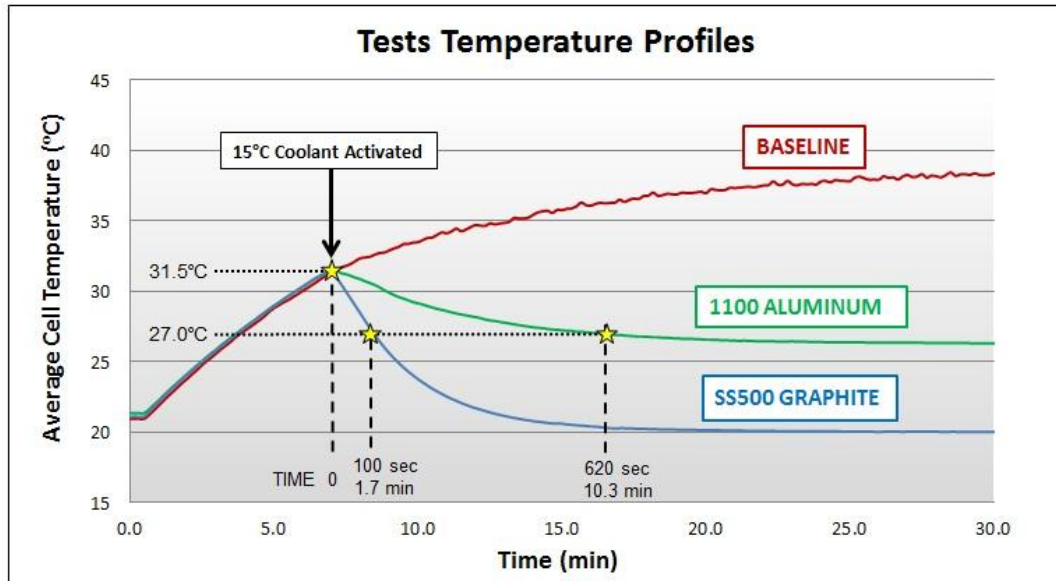


Figure 12: Results of GrafTech simulated battery cooling experiment^[2]

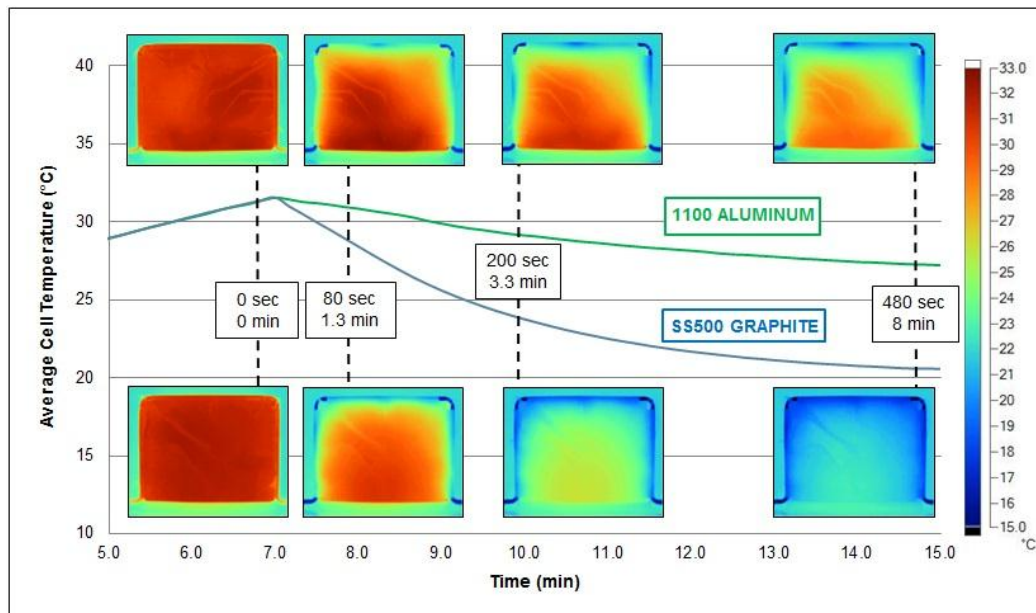


Figure 13: Thermographs of GrafTech simulated battery cooling experiment^[2]

The graphs and pictures clearly show that the graphite heat spreaders outperform the aluminum. In reaching a target temperature of 27°C from 31.5°C, GrafTech states that the graphite solution reaches the target temperature 80% faster than the aluminum solution. In addition the graphite provided a 27% higher heat

transfer coefficient, decreased temperature gradients by 25% under steady-state conditions and 48% under transient conditions. Clearly the graphite material showed promise in removing heat from the simulated battery packs when used in conjunction with a liquid cooling system. More study was needed, however, to see if this performance would be seen using actual battery packs with passive cooling systems.

3.2 Center for Automotive Research at The Ohio State University

The investigation into using graphite heat spreaders in lithium-ion thermal management systems was continued at CAR by Hussam Khasawneh under the direction of Dr.s Marcello Canova and Yann Guezennec. This work entailed studying the effects of graphite heat spreaders on battery packs constructed of A123-ANR26650 lithium-ion cells. Three packs were constructed with the cells configured in two rows of five cells each and wired in series as shown in figure 14 below.



Figure 14: Battery pack configuration

This configuration is often used in modern-day commercial hand-held power tools. Three different variations of this design were constructed: a control pack with no cooling, one with the graphite heat spreaders, and one with the graphite heat spreaders and an aluminum heat sink. Each of these pack designs were also simulated using COMSOL Multiphysics® FEM software. Both the simulated and experimental cells were subjected to a several duty cycles comprised of a current vs. time profile consistent with hand-held power tool use. The resulting temperatures and temperature gradients were compared between the different pack configurations, and between the experimental and simulated trials. Figure 15 below shows a comparison of the temperatures at several points in the battery pack vs. time between the experimental and simulated results. A strong correlation is shown.

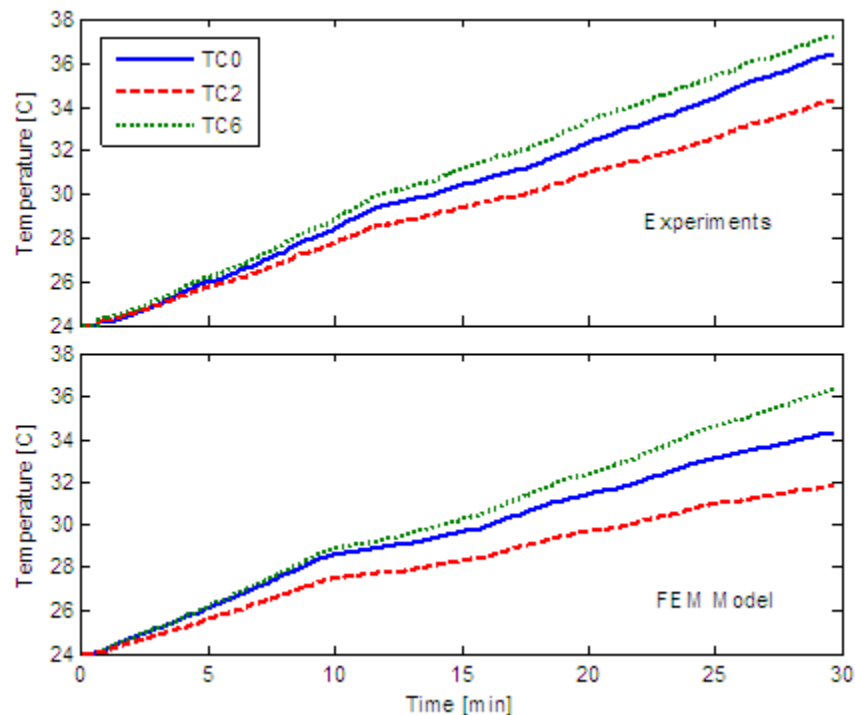


Figure 15: Comparison of experimental (top) and predicted (bottom) temperatures at different locations in the pack^[1]

Figure 16 below shows thermographs for the simulated and experimental packs (using an infrared camera). Please note that the temperature scale for the experimental thermograph is an estimate.

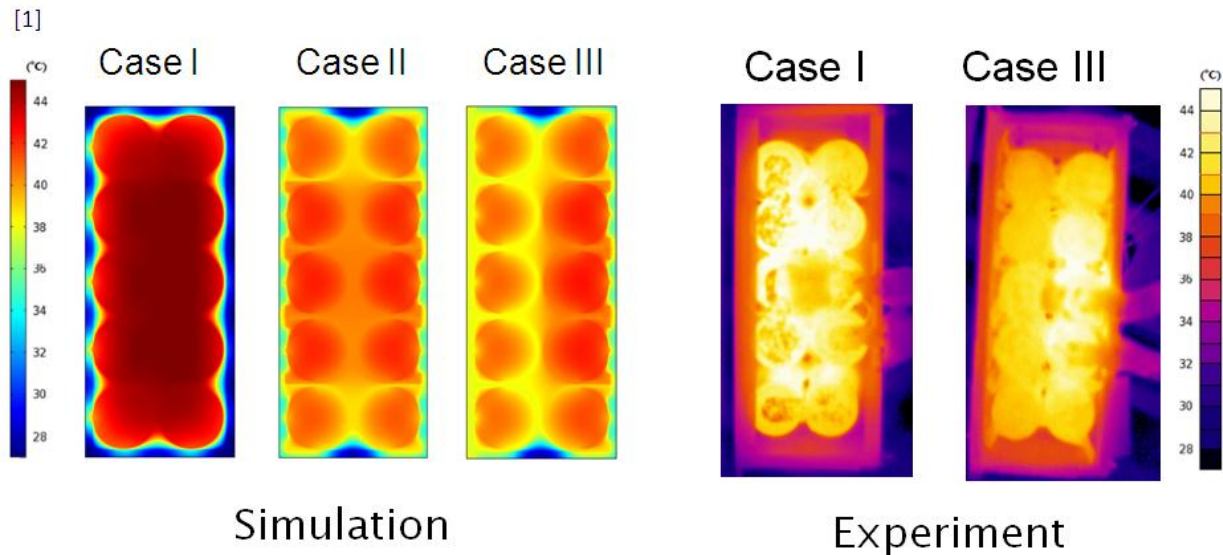


Figure 16: Thermograph comparison between simulated and experimental results^[1]

The study served both to validate the COMSOL thermal FEA simulation and to demonstrate the effectiveness of flexible graphite heat spreaders as a passive solution to lithium-ion battery thermal management. Further work was suggested at the time to evaluate the effect of this thermal management on actual battery performance and endurance.

Chapter 4: Methods and Procedure

4.1: Experiment Overview

As a continuation of the experiments previously performed at CAR, it was decided to evaluate the actual performance and endurance benefits that might be gained using flexible graphite heat spreaders as a thermal management solution for lithium-ion battery packs. To this end, an experiment was designed in which three battery packs would be cycled repeatedly while the voltage and temperature balance within the packs was tracked. If the flexible graphite was effective in promoting cell balance and endurance, then as the packs age, the voltage and temperature imbalance increase in the control battery pack should gradually outpace the unbalance in the packs with the flexible graphite.

The battery pack design from the previous CAR experiments was retained, having ten A123-ANR26650 cells wired in series in a two by five configuration. These cells are lithium-ion phosphate based with a 3.3V nominal cell voltage with a capacity of 2300 mAh. Figure 17 below shows the cell and extended specifications.

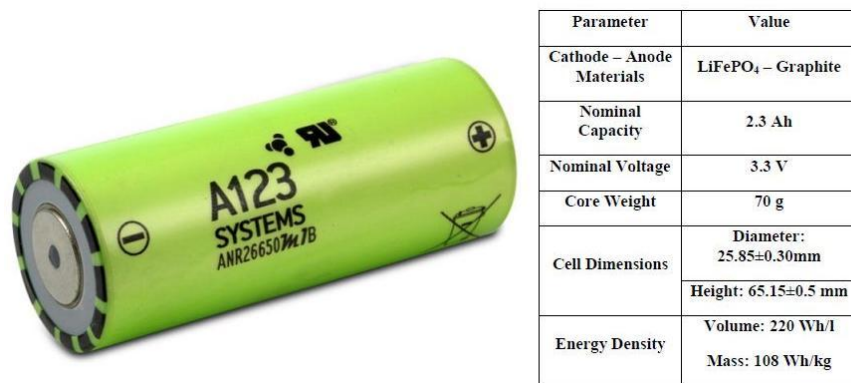


Figure 17: A123 cell and specifications⁵

⁵ <http://www.a123systems.com/collateral/Images/English-US/26650.jpg>

The graphite material is GrafTech's Spreadershield™ SS-400 flexible graphite with a range of in-plane thermal conductivity of 360-420 W/mK. Three battery packs were to be tested including a control with no thermal management, and two packs with separate heat spreader configurations. During pack construction, however, a problem arose with the original pack design.

4.2: Problems with Original Pack Design

A significant problem was discovered with the original battery packs. The flexible graphite heat spreaders were detaching from the cells and from the heat sink. Figure 18 below shows the graphite material peeling away from the pack surfaces.

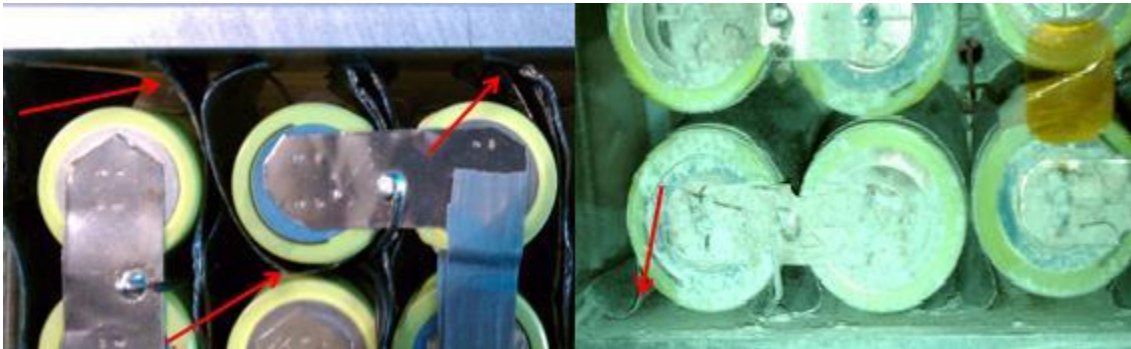


Figure 18: Arrows showing flexible graphite adhesive failure

Three possible causes exist for this failure. The graphite material supplied by GrafTech was a slightly thicker stock than some of the original material, and may have exerted a greater force on the adhesive bonds where the curved profiles tried to straighten back out flat. Even the original graphite material was beginning to peel however. This may have been due to either dirty cell and heat sink surfaces, or to heating and cooling cycles gradually weakening the adhesive.

Whatever the reason, the failing adhesive caused the graphite material to come away from the cells and the heat sink, lessening the available surface area through which to conduct heat away from the cells. A solution was needed to keep the graphite in close contact with the cells and make sure the contact remained tight throughout the testing process. To achieve this goal, a new battery pack case was designed and constructed.

4.3: Design and Construction of New Packs

The new design implemented a solid piece of gray PVC plastic that was machined to closely fit the contour of the cells in their pack configuration. Figure 19 below shows the CAD model of the proposed pack design with the cells and graphite installed.

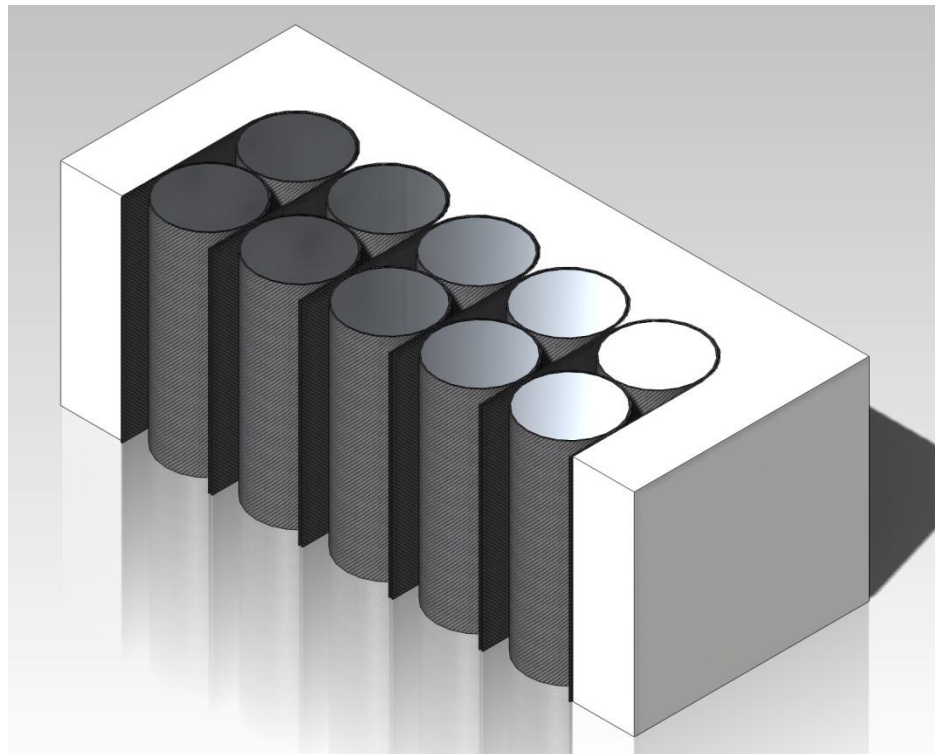


Figure 19: CAD model of new battery pack design

The heat sink is not shown in the model, but will bolt onto the end where the exposed cells are seen. The pack compresses the cells and graphite together and will hold the graphite material in close contact with the cells and the heat sink, even if the adhesive begins to weaken. Figure 20 below shows the components of the pack laid out prior to assembly.



Figure 20: Components of new battery pack design

Because the old packs were completely disassembled, (excepting the control pack which does not have any thermal management) the opportunity was taken to redesign the geometries of the heat spreader material. Figure 21 below shows the routing paths of the flexible graphite between the cells of the battery pack.

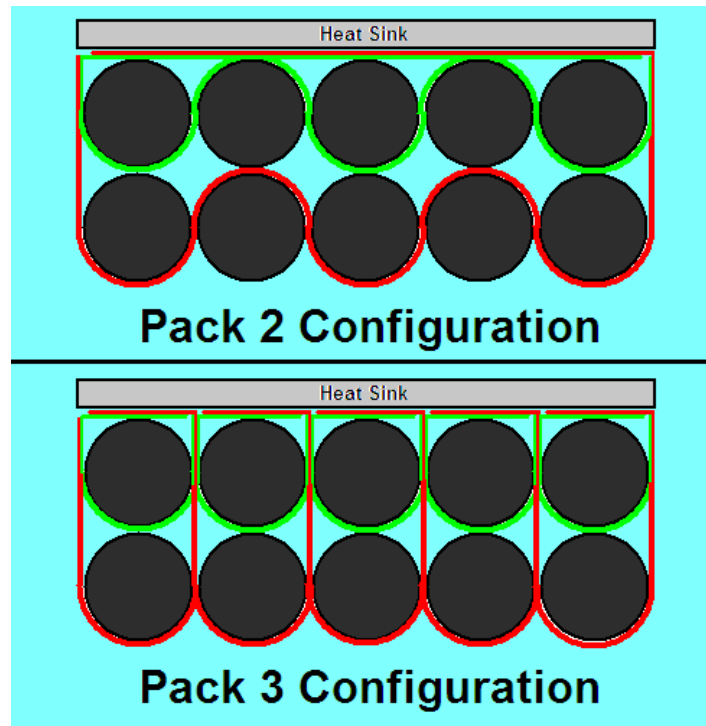


Figure 21: Routing of graphite material

In this diagram the red and green contours show the paths of the flexible graphite for the bottom and top cells respectively.

As can be seen, the heat spreading system of pack two consists of two pieces of the flexible graphite material. One piece snakes back and forth between the top row of cells, and the other snakes between the bottom row of cells. While going between the cells, both pieces of graphite are the same width as the height of the cells. Where the strips come up to fold over and make contact with the heat sink, they are split to half their width so that the strips for the top and bottom cells can share equal contact area with the heat sink. Figure 22 shows a top view of pack 2 as it's being assembled, just prior to the heat sink being bolted down. The brown backing of the graphite material seen in the photo was then peeled and the strips laid down flat across the tops of the cells, followed by the addition of the heat sink.



Figure 22: Top view of pack 2 prior to heat sink addition

The heat sink compressed the entire assembly as it is tighten on with the bolts assuring good thermal contact between all surfaces.

The heat spreading system of pack three consists of ten different pieces of the flexible graphite material. Referring back to figure 21, five strips form horseshoe loops around the bottom cells, and five strips similarly wrap around the top cells. The strips are the full width of the battery height as in pack two until they come up to meet the heat sink. They are then trimmed down to half this width and bent over in a staggered pattern so that each set of strips shares an equal area of the heat sink. A view of pack three just prior to heat sink installation is shown below in figure 23.

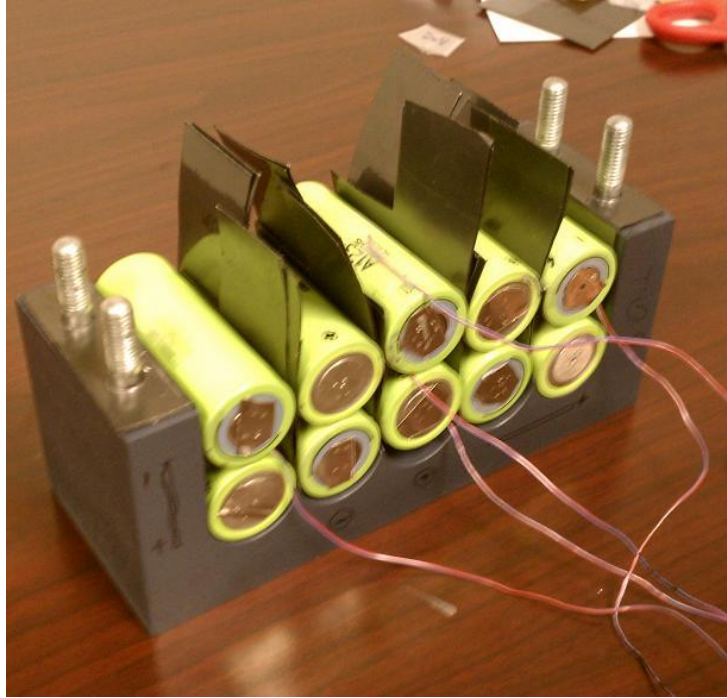


Figure 23: Top view of pack 3 heat spreaders

For instrumenting the battery packs, both were fitted with 7 thermocouples at different locations in the packs. The locations are shown below in figure 24.

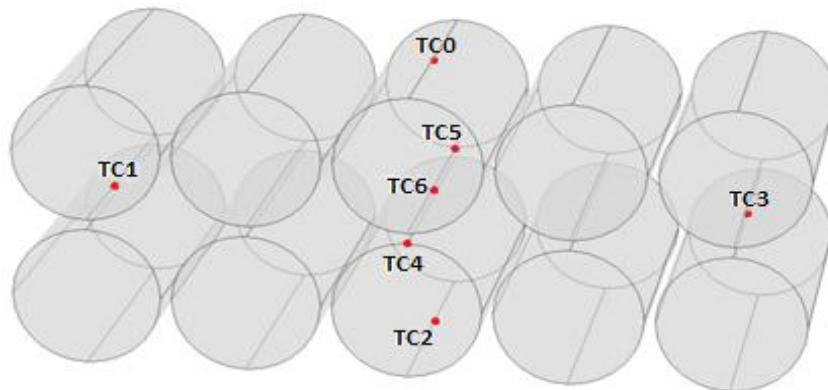


Figure 24: Locations of battery pack thermocouples

In addition, voltage leads were then attached to each individual cell so that the voltages of each cell could be monitored, both for experimental data and for safety sake when charging and discharging the cells.

A completed cell is shown below in figure 28 fully instrumented and connected to the testing apparatus.

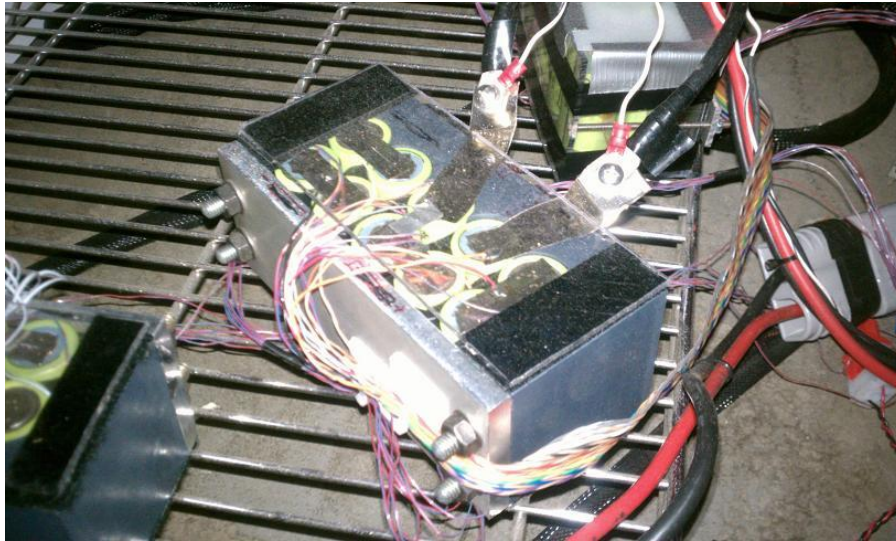


Figure 25: Completed test pack connected to testing setup

4.4: Testing apparatus

The testing apparatus consisted of two primary components. The first was a battery tester whose function it was to run a program which would subject the battery packs to a specified current profile during both charging and discharging. The tester also tracked current and total pack voltages during cycling. The second component was a data acquisition setup whose function was to collect more precise data on the battery packs. It tracked ten voltages (one for each cell) and 7 thermocouple data streams for each battery pack, for a total of 51 total channels of data. The data acquisition setup also recorded this data for later analysis and also alerted the operator and battery testing module to out-of-bounds operation.

The battery tester used was a Maccor battery tester. This tester is capable of testing eight battery packs simultaneously and independently, although for this

experiment only three of the channels were needed. Figure 26 below shows the Maccor battery tester.



Figure 26: Maccor battery testing system

The Maccor is operated by a PC running proprietary software which allows a program to be written to deliver a specific current profile to the battery pack. The Maccor is also capable of altering or terminating the program based on the total battery pack voltage. Figure 27 below shows the GUI of the Maccor Tester monitoring the current flow in each pack.

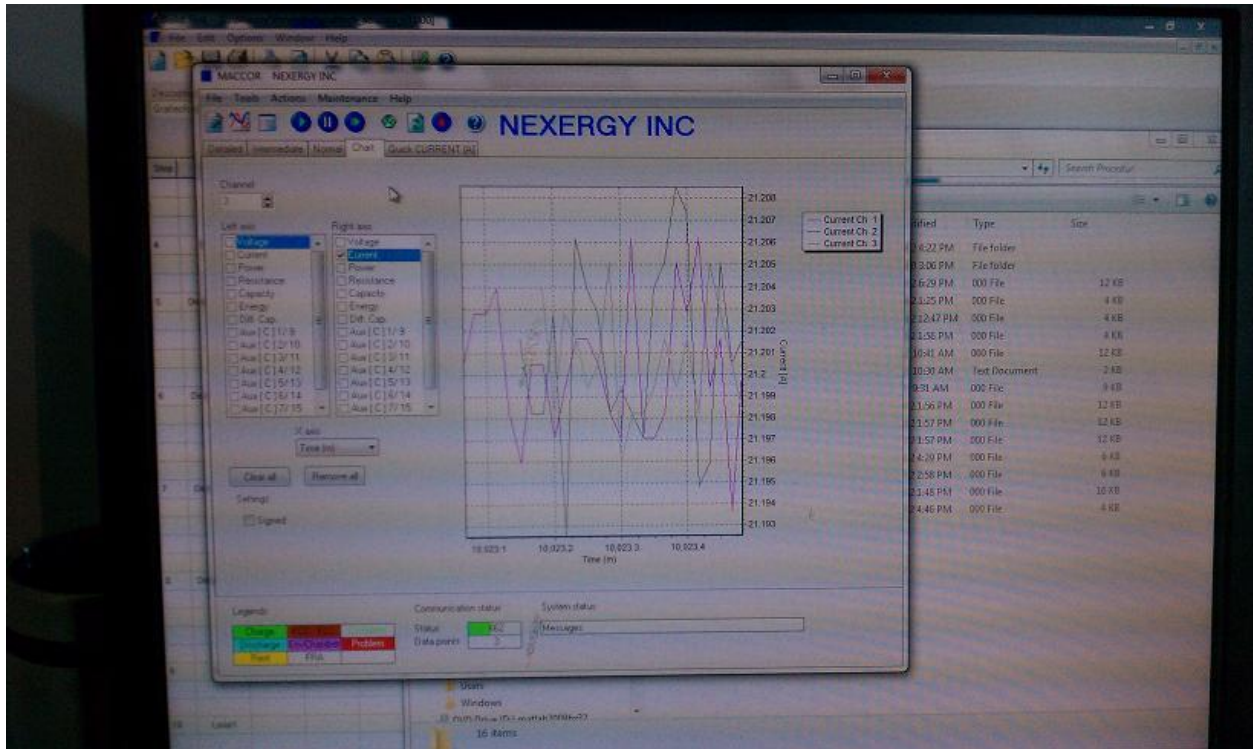


Figure 27: User interface for Maccor tester

The data acquisition system consisted of a multi-channel data acquisition board connected to another PC running National Instruments LabVIEW software. The data acquisition system collected all 51 data streams from the battery pack instrumentation. The data was displayed and recorded as lvm files for later analysis and processing. The data acquisition system was also capable of communicating to the Maccor system by means of a controller area network (CAN) bus. This allowed the battery cycling process to be terminated autonomously in the case of an out of bounds temperature or voltage signal from any one of the monitored 51 channels. Figure 28 shows the LabVIEW main page for the data acquisition interface.

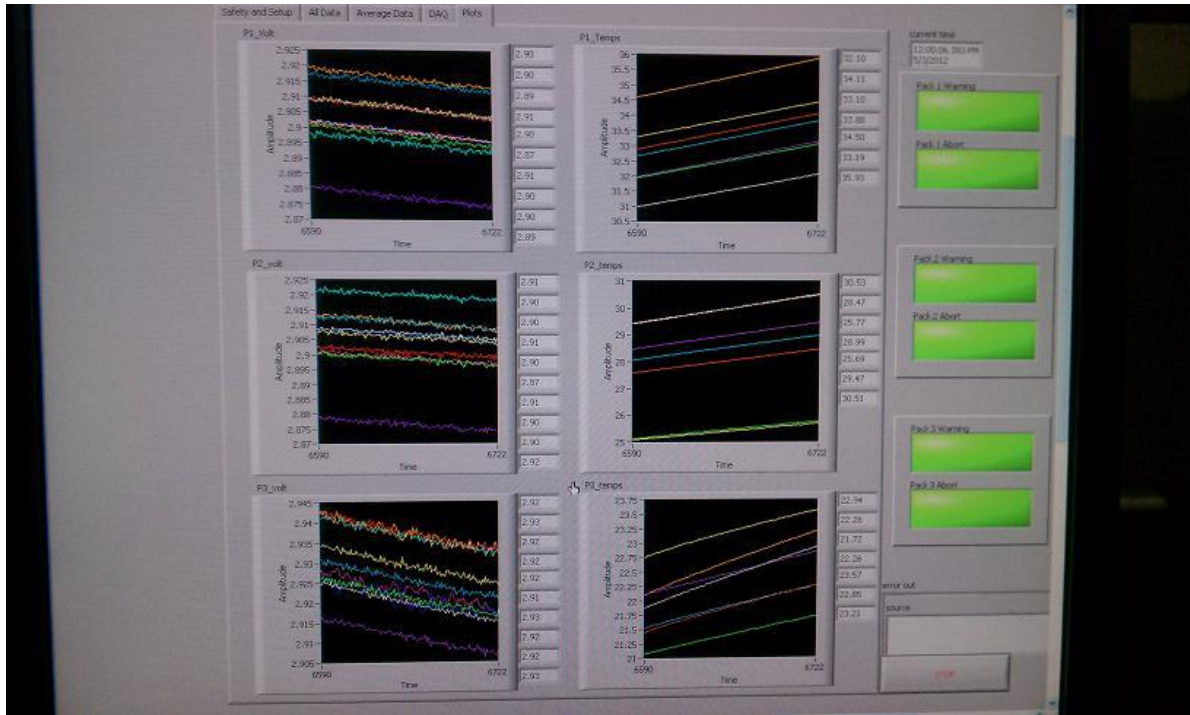


Figure 28: User interface for the data acquisition system

The data acquisition system and the battery tester system ran essentially independently. The Maccor PC gave instructions to the Maccor tester to dictate current flow conditions. The Maccor ran this current through the pack to either charge or discharge the pack, and also read the overall pack voltage and current. This data was relayed back to the Maccor PC, where it was displayed on the monitor, logged, and also fed to the current program algorithm. The data acquisition board took the signals from the thermocouples and cell voltage sense leads and fed them to the data acquisition PC, where the data was displayed and logged. The only communication between the data acquisition system and the battery tester was over the CAN bus, where the data acquisition PC could send error flags to the Maccor in case any one cell or thermocouple went outside allowable limits. A summary of the overall data flow is shown below in figure 29.

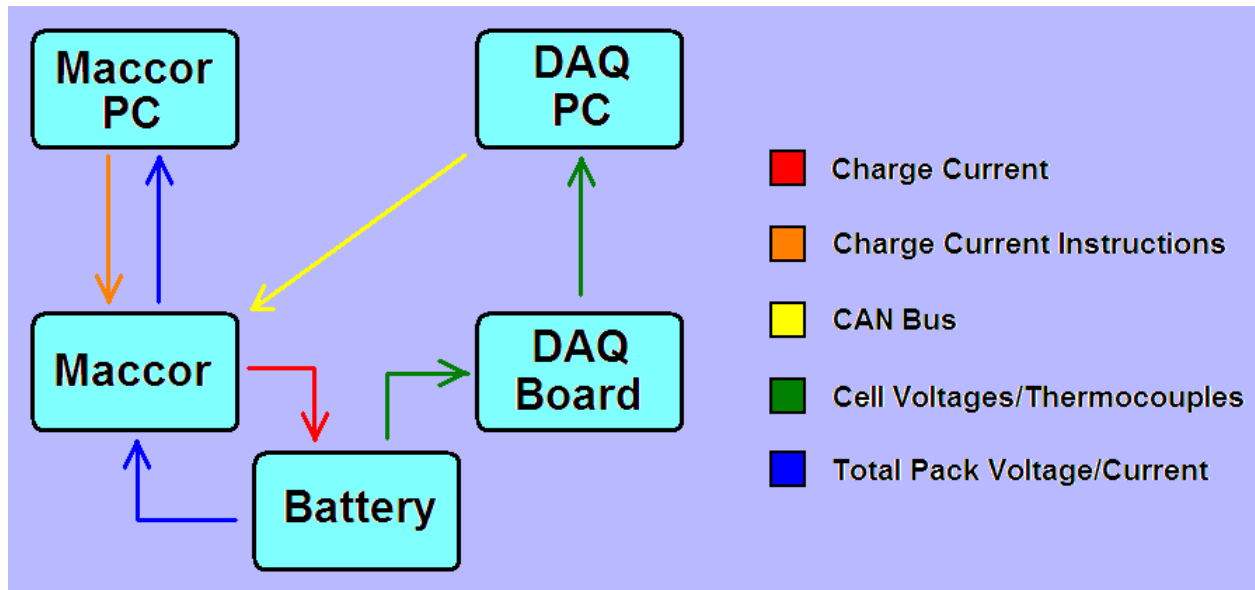


Figure 29: Overall system data flow

All three battery packs were cycled simultaneously by this system. Figure 30 below shows a picture of the entire experiment. The DAQ computer is on the left, the Maccor computer is on the right. The packs are located behind the Maccor towers. Graduate student Hussam Khasawneh is also shown looking surprised.



Figure 30: Image of complete experimental setup

4.5: Testing Parameters

The parameters of the test were modeled after simulated use of a hand-held power tool. The cells were subjected first to a light current discharge profile for a number of cycles until the system was determined to be functioning properly. After this, a more abusive charge cycle was used, which drained the batteries at a much higher current. This would not only reduce the time needed for one complete cycle, but would also age the packs faster resulting in a fewer number of cycles needed before results were seen.

The light current discharge profile consisted of a 6.5 amp discharge (3C rate) for 75 seconds (1.25 minutes) followed by a 4.5 amp discharge (2C rate) for 1425 seconds (23.75 minutes). A plot of the current If the pack voltage dropped below 20 volts, or if any individual cell dropped below 2 volts, the discharge was stopped and the pack was allowed to rest for two minutes before a one C constant current charge (2.3A) until the pack reached 37 volts or any individual cell reached 3.7 volts. This was followed by another two minute rest. If the exit conditions for pack imbalance were not met, the cycle was repeated. A flow chart of the charge/discharge cycle is shown below in figure 31.

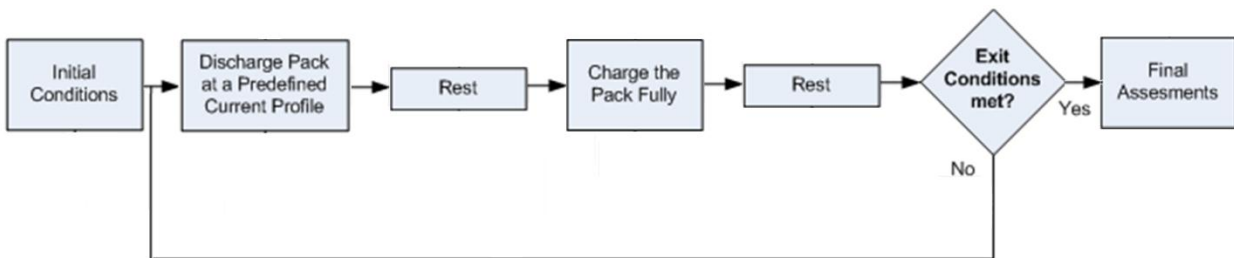


Figure 31: Charge/discharge cycle flowchart⁶

⁶ Courtesy of John Neal

The medium discharge cycle followed the same structure as the light discharge cycle, except that a discharge rates of 6C and 4C were used.

The exit conditions were based off the imbalance inside each of the battery packs. As the battery packs became more and more imbalanced, the deviations in the voltages and the thermocouple signals increased. Four metrics were looked at to determine the extent of this deviation. The first two were the standard deviation of the cell voltages and thermocouples. The second two were the difference between the maximum and minimum voltage and thermocouple signals respectively. The choice for exit condition values for these parameters will be determined after initial observations of the battery packs reactions to the cycling process.

Chapter 5: Results

Although the experiment is still in the earlier testing stages, some preliminary data has been obtained. Some sample results are shown below. Again the key metrics are cell voltage standard deviation and maximum difference, and thermocouple standard deviation and maximum difference.

Figure 32 shows a plot of the maximum cell difference as a function of time.

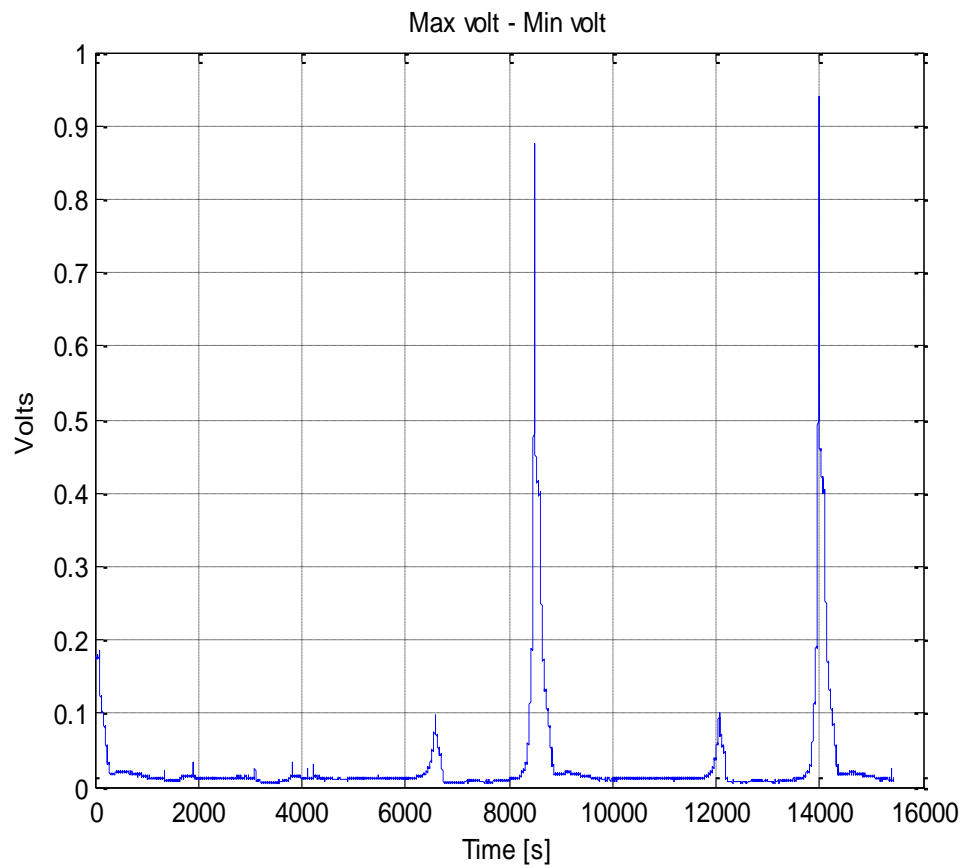


Figure 32: Maximum cell difference vs. time⁷

The tall peaks around 9000 and 14000 seconds represent the end of a discharge cycle, where the cells are nearly drained and the cell voltages are very sensitive to changes in charge. In order to get a fair measurement of charge imbalance, the cell imbalance for

⁷ Courtesy of John Neal

a given cycle is averaged over the entire cycle. In the plot above, this is around forty millivolts.

Figure 33 below shows the standard deviation of the cell voltages for the same cycles as a function of time.

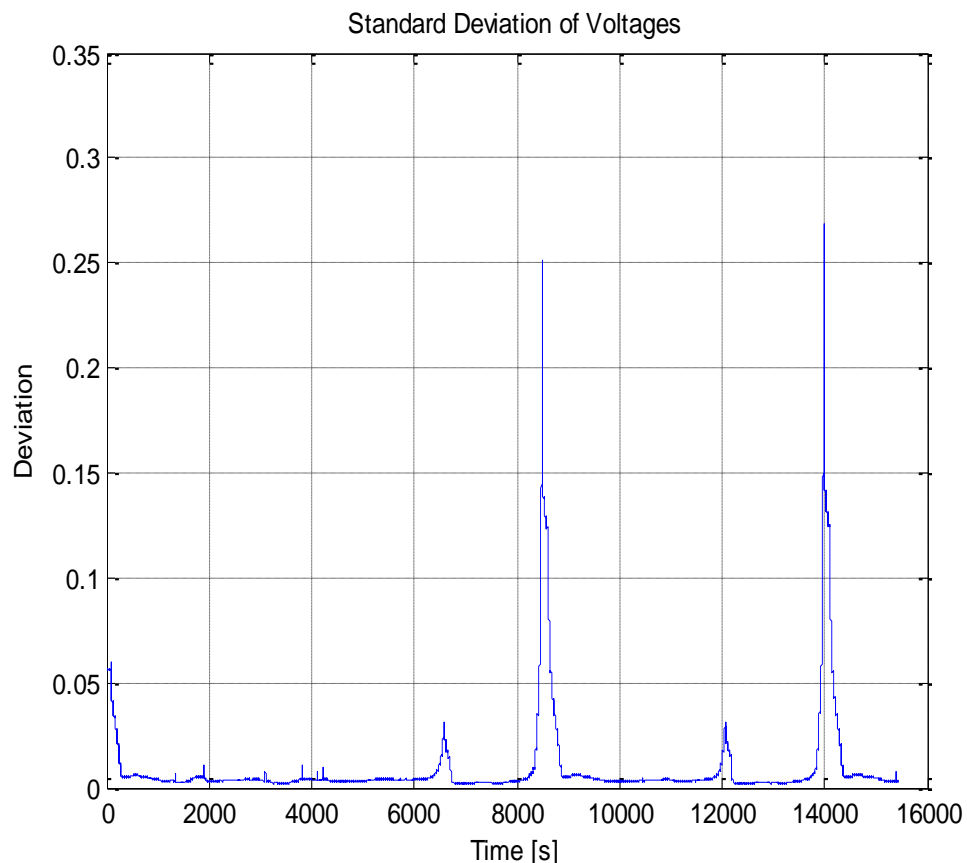


Figure 33: Cell standard deviation as a function of time⁸

As can be seen, the contours of the two plots appears very similar, as is expected as both standard deviation and maximum cell difference both are a measure of disparity in the cell voltages. Again, the peaks occur at the end of the discharge cycle, and the unbalance for a cycle is read just prior to the start of the discharge cycle. In this case around 20 millivolts.

⁸ Courtesy of John Neal

Figure 34 below shows a plot of the maximum thermocouple distance as a function of time for the same cycles as the above voltage plots.

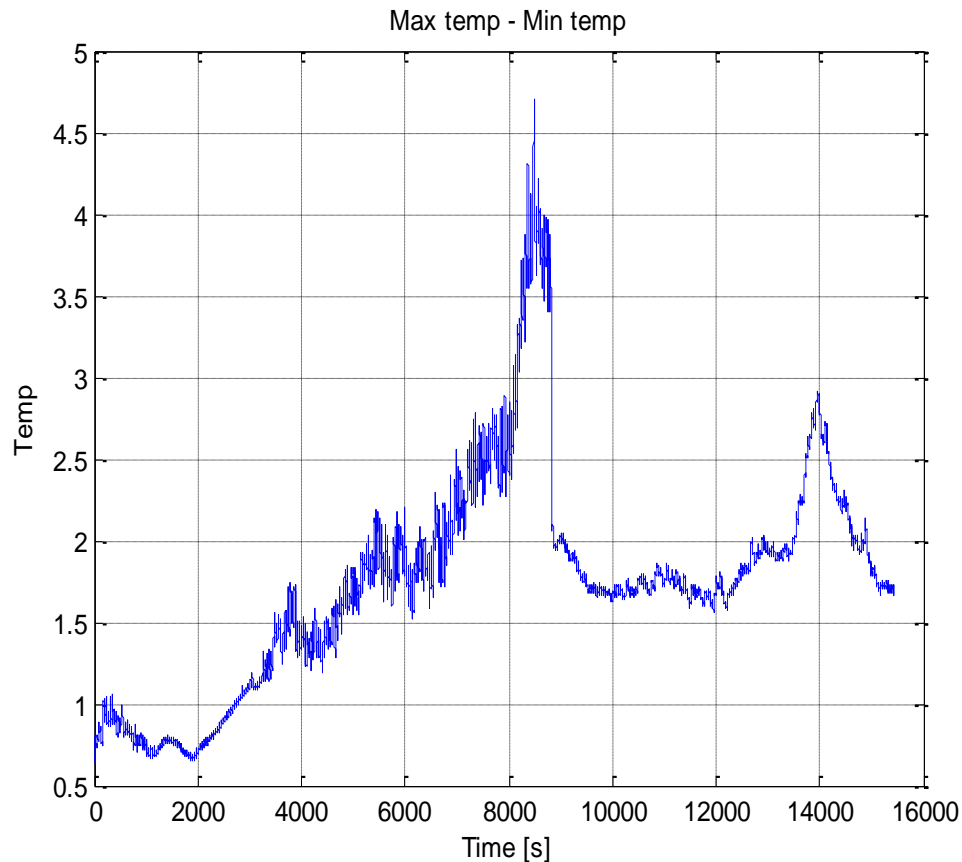


Figure 34: Plot of the maximum thermocouple difference as a function of time⁹

Although the thermocouple plot does not resemble the voltage plots, the trends are still the same in that the temperature differences between the thermocouple locations increase as the packs near the end of discharge. Because temperature ages cells throughout the cycling of the pack, the temperature imbalance is read as the average temperature difference throughout the entire cycle. For the second cycle above, this average temperature maximum difference is around 2.4°C.

⁹ Courtesy of John Neal

Figure 35 below shows a plot of the thermocouple standard deviation, again for the same cycles as the other plots.

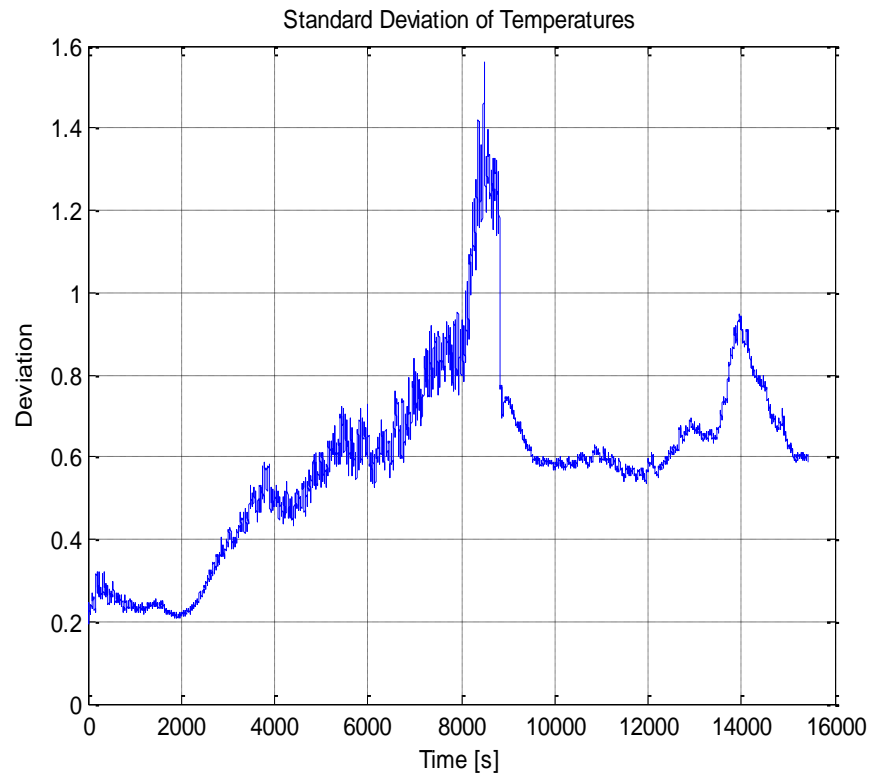


Figure 35: Plot of the thermocouple standard deviation as a function of time¹⁰

As with the voltage plots, the maximum thermocouple difference and thermocouple standard deviation plots are very similar. The thermocouple standard deviation is read in the same way as the maximum thermocouple difference in that the average is taken over the entire cycle. In this case, the value is around 0.8°C.

By looking at the trend of these battery pack unbalance metrics as a function of the cycle number, the aging of the battery can be visualized. As of the completion of this paper, a series of seven cycles have been completed. The raw data of the voltage and temperature traces for pack one are shown below in figures 36 and 37.

¹⁰ Courtesy of John Neal

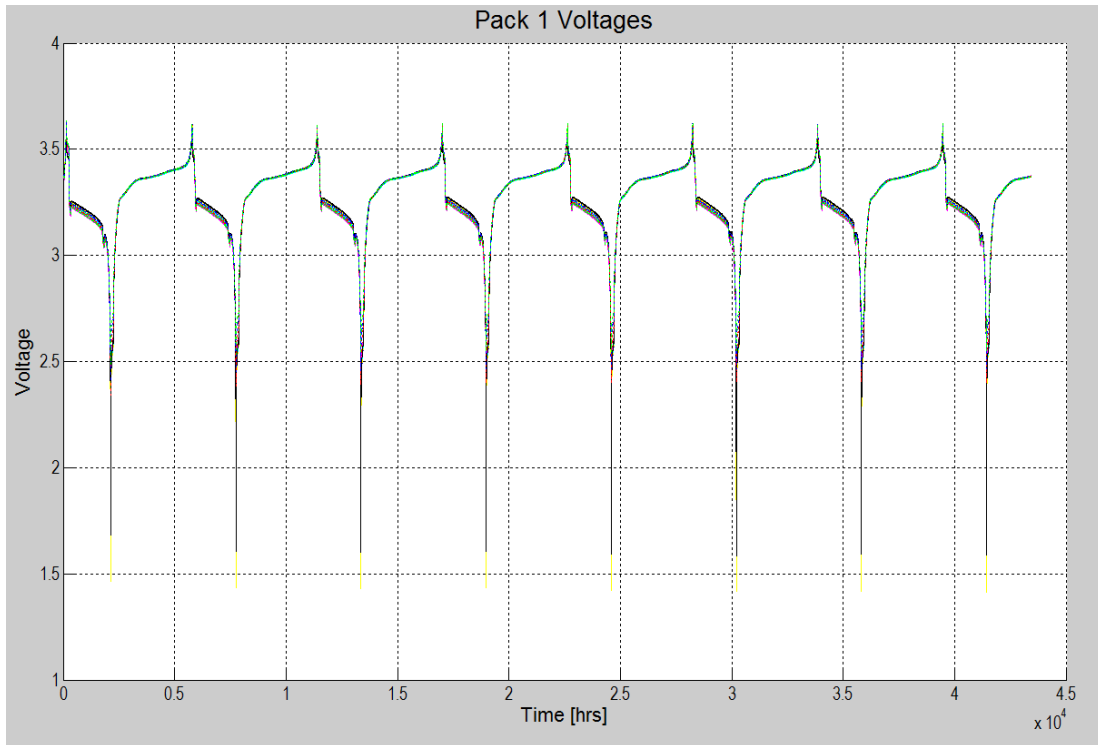


Figure 36: Pack 1 voltage traces for preliminary 7 cycles

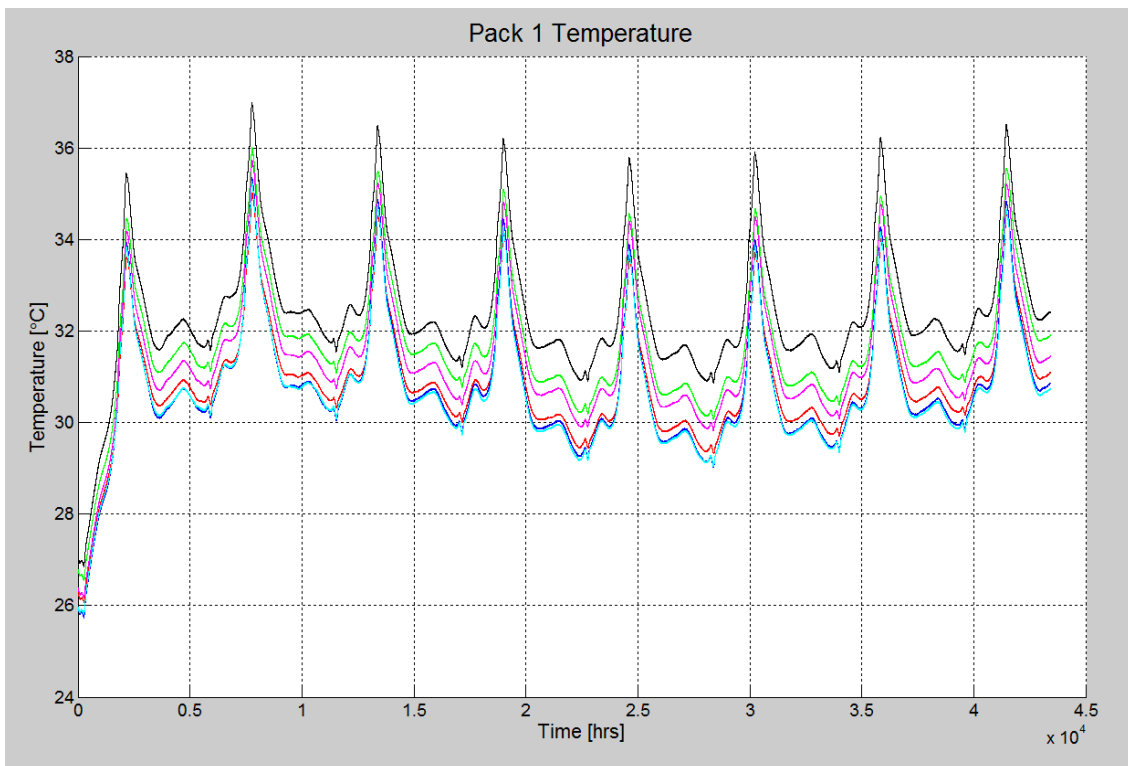


Figure 37: Pack 1 temperature traces for preliminary 7 cycles

From this raw data, the averages of the maximum voltage and temperature difference were computed for each cycle. The results for the voltage imbalance in all three packs are shown below in figure 38.

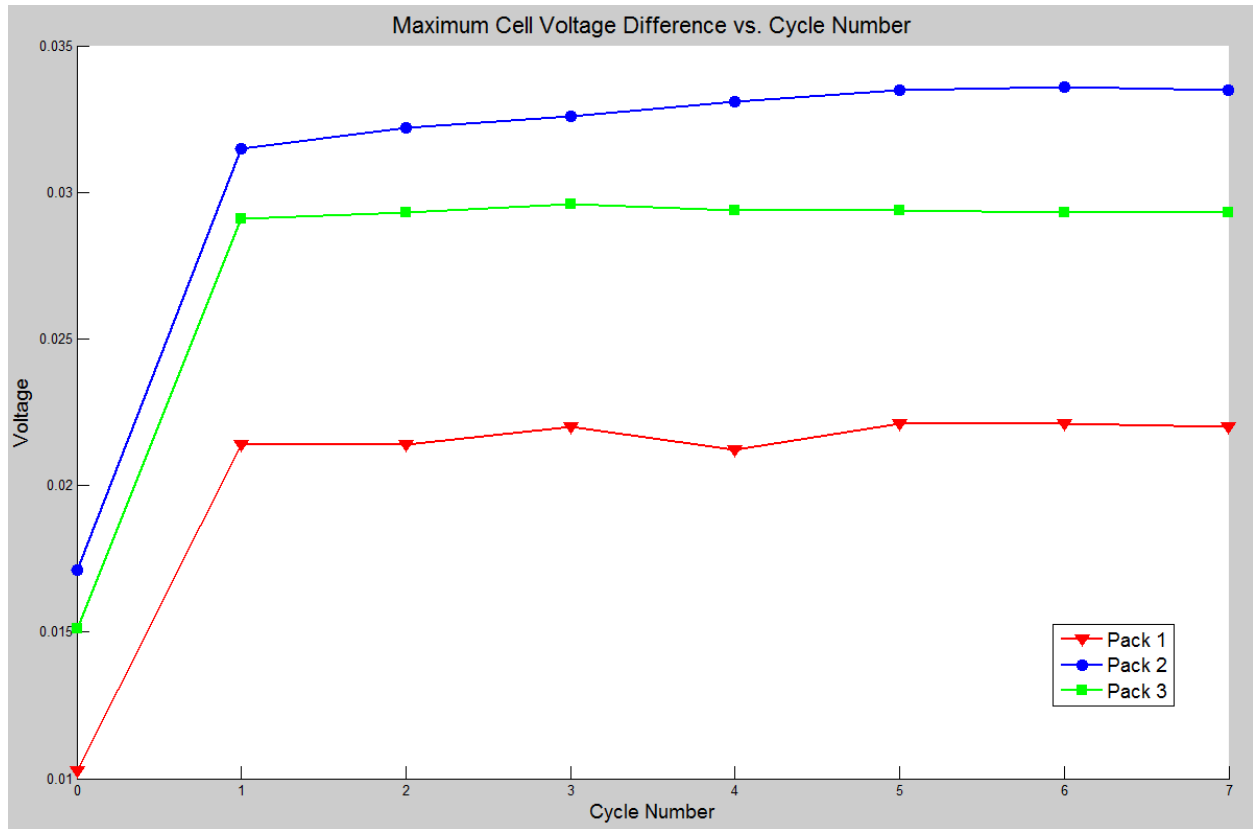


Figure 38: Maximum cell voltage difference vs. cycle for all three packs

Unfortunately, not enough cycles have been run yet for a trend to emerge from this data. Pack one maximum voltage imbalance only increase by 0.6 mV over the 7 cycles, where pack two increases by 2mV, and pack three by 0.2 mV. This fluctuation is presumed to be in the noise of the experiment. Hopefully, after many more hundreds of cycles are run, the data will show the curve for pack one increasing at a greater rate than packs two and three.

A plot of the temperature imbalance in the cells for all three packs is shown below in figure 39.

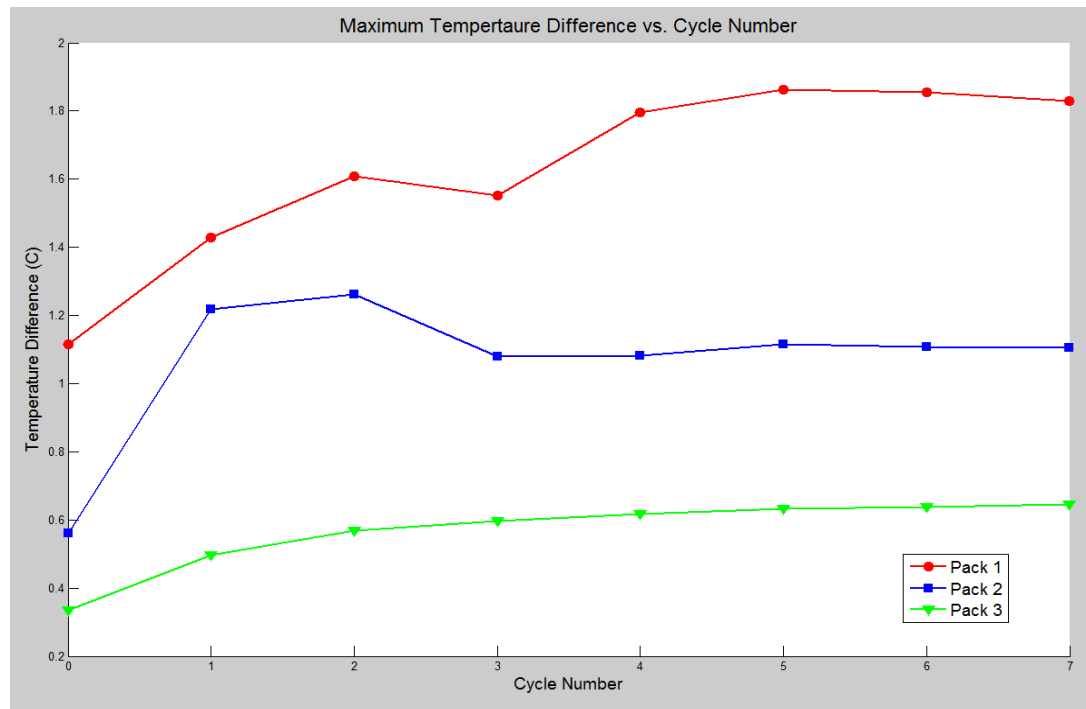


Figure 39: Maximum temperature imbalance for all packs

This data is slightly more promising. The data shows that the temperature imbalance in pack one is higher than packs two and three right from the beginning. Additionally, even over seven cycles, there appears to be a much greater rate of increase in imbalance per cycle in pack one than in packs two and three. Pack one's imbalance increases by around 0.40°C over the seven cycles, pack three shows an increase of only 0.15°C , and pack two actually shows a decrease in imbalance of 0.12°C . Because the aging of the cells is dependent on temperature, this increasing temperature imbalance should lead to the voltage imbalance expected as more cycles are run. While it is far too early in the experiment to call this a positive result, it certainly is promising initial data.

Chapter 6: Conclusion

6.1: Contributions:

The purpose of this research was to evaluate the efficacy of a flexible graphite thermal management system in enhancing the performance and endurance of lithium-ion battery packs. My research accomplished this by constructing several battery packs and then cycling them while tracking data regarding cell imbalance and performance over the life of the packs. The data shows not only that the flexible graphite can reduce the temperature imbalance in the packs, but it appears to show that the increase in this imbalance as the packs are cycled is slowed when the flexible graphite is used. While there is yet not enough data to show the graphite's effect on voltage imbalance reduction, the temperature imbalance improvement gives strong reason to believe that this effect will be seen as the experiment progresses and more cycles are completed.

6.2: Future Work:

There is still much work that needs to be done. In addition to completing the mild cycle experiment until exit conditions are met, there are other avenues of performance that might be explored. Cell capacity as a function of cycle number might be calculated as an additional metric of battery performance. This might be a more useful metric as it is a direct measure of how long the battery can last in a given application.

Other areas that might be explored include testing the flexible graphite material in prismatic battery packs. These packs are made of cells consisting of thin, flat foil pouches whose geometry would permit ease of pack construction as well as nearly 100% cell surface coverage of the flexible graphite heat spreaders. The cooling effect

would presumably be more pronounced so results should be seen sooner than the current experiment using cylindrical cells. In addition, these cells are becoming more of a dominant cell and pack geometry as time progresses.

6.3: Summary

This thesis detailed experiments being performed at CAR to evaluate the usefulness of flexible graphite heat spreaders in increasing lithium-ion battery pack endurance and performance. Three battery packs were constructed, two of which incorporated flexible graphite heat spreaders and one control pack was made without them. The cells were charged and discharged over several cycles, and the average voltage and temperature imbalance examined as an indicator of battery aging. While there was not enough data as yet to detect a significant slowdown in voltage imbalance increase, there did appear to be a reduction in the rate of increase in temperature imbalance by using the graphite heat spreaders that should lead to an improvement in endurance as the experiment progresses.

References

- 1.) H. Khasawneh - Analysis of Heat-Spreading Thermal Management Solutions for Lithium-Ion Batteries, Master's Thesis, 2011
- 2.) J. Taylor, R. Wayne, M. Smalc, J. Norley, "Active Thermal Management of Lithium Ion Batteries Using Flexible Graphite Heat Spreaders", GrafTech Presentation, 2011
- 3.) H. Khasawneh, J. Neal, M. Canova, Y. Guezennec, "Analysis of Heat-Spreading Thermal Management Solutions for Lithium-Ion Batteries", Proceedings of the ASME 2011 International Mechanical Engineering Congress & Exposition IMECE2011, November 11-17, 2011
- 4.) T.R. Crompton, "Battery Reference Book", Newnes, Woburn, Massachusetts, 2000
- 5.) M. Wakihara, O. Yamamoto, "Lithium Ion Batteries Fundamentals and Performance", Wiley-VCH, 1998